Journal of the Serbian Chemical Society
JSCS@tmf.bg.ac.rs • www.shd.org.rs/JSCS
*J. Serb. Chem. Soc.* *83* (9) 1031–1045 (2018)
*JSCS–5131*
UDC 66.046.58:66.065.5:66.099.2:544.362:549
*Original scientific paper*

# Study on the mineralogical crystallization of granulation of gas-quenched blast furnace slag

KANG YUE[1]*, LIU CHAO[1], ZHANG YUZHU[1,2], XING HONGWEI[2], LONG YUE[2] and JIANG MAOFA[1]

[1]*School of Metallurgy, Northeastern University, 110819, Shenyang, China and* [2]*College of Metallurgy and Energy, North China University of Science and Technology, 063009, Tangshan, China*

(Received 12 December 2017, revised 22 May, accepted 31 May 2018)

*Abstract*: The process of granulation in blast furnace slag (BFS) by gas quenching can effectively recover the waste heat of BFS and improve the value-added nature of the BFS byproduct. With decreasing temperature, BFS crystallizes into melilite, anorthite, spinel, *etc*. Mineral crystallization, however, is not conducive to the production of amorphous BFS beads. This study uses thermodynamic simulation and remelting experiments to study the influences of basicity, acidity, and the MgO and $Al_2O_3$ content of the BFS on the crystallization. By controlling the composition of the BFS, mineral crystallization in the process of granulation in BFS, by gas quenching, could be prevented. The results show that increasing the basicity of the BFS causes the mineral crystallization temperature to increase rapidly. The mineral phase then crystallizes at a higher temperature, which is not conducive to the formation of an amorphous phase. Increasing the acidity of the BFS can greatly decrease the crystallization temperature, *e.g.*, when the acidity increases to 1.3, amorphous BFS beads can be obtained at the gas quenching temperature (1623 K). Although increasing the MgO and $Al_2O_3$ contents in the BFS had little effect on the crystallization temperature and yield, the preparation of amorphous BFS beads by gas quenching could be realized by adjusting the acidity of the BFS.

*Keywords*: blast furnace slag; crystallization; simulation; granulation; acidity.

## INTRODUCTION

Blast furnace slag (BFS) is the main byproduct of iron production and is produced at a rate of 300–350 kg $t^{-1}$ taking away about $1.5\times10^6$ kJ $t^{-1}$ of sensible heat. Currently, traditional water quenching wastes a large amount of water and pollutes the environment. The temperature of the water used for slag washing is about 336–353 K[1–3] and the efficiency of the waste heat recovery is less than 10 %.

* Corresponding author. E-mail: kang-kai-yue@163.com
https://doi.org/10.2298/JSC121217051Y

The process of bead-forming in BFS by gas quenching has great practical significance; it can efficiently recover the sensible heat of the BFS and turn the BFS into a high value-added byproduct. Simultaneously, this process can allow the iron and steel industry to reduce high-energy emissions and utilize much more of the solid waste.[4–6]

Many studies on the treatment methods for BFS and waste heat recovery have been performed. Liu[7] *et al.* studied a dry granulation method for rotary cups, which not only recycles the sensible heat of BFS but also saves a large amount of fresh water and does not pollute the environment. Zhu[8] *et al.* studied a granulation technique combining a high-speed rotating cup with blast air. The effects of the rotating speed of the atomizer, liquid flow rate, and the blast air flow rate on the particle size, particle mass distribution and fiber mass fraction were studied. Pickering[9] *et al.* proposed a new process of dry granulation and waste heat recovery of BFS, which could recover 60 % of the waste heat energy. This study uses thermodynamic simulations and experiments to explore the influence of the BFS composition on mineral crystallization and crystallization temperature, which improves the bead-forming process in BFS by gas quenching and provides a theoretical basis for the granulation process in BFS by gas quenching.

## EXPERIMENTAL

### *Experimental materials*

The raw BFS was provided by an iron plant. The slag temperature was 1723 K and the main chemical composition of the BFS is shown in Table I. CaO, $SiO_2$, MgO and $Al_2O_3$ analytical reagents were used as the conditioning agent.

TABLE I. Chemical composition of the blast furnace slag

| Composition | $SiO_2$ | CaO | MgO | $Al_2O_3$ | $Fe_2O_3$ | $TiO_2$ | $K_2O$ | $Na_2O$ | MnO |
|---|---|---|---|---|---|---|---|---|---|
| Content, % | 33.53 | 36.25 | 8.64 | 15.82 | 1.57 | 1.38 | 0.54 | 0.32 | 0.17 |

The basicity and acidity of the BFS in these experiments was 0.91 and 1.1, respectively, and the influence of basicity, acidity, and the MgO and $Al_2O_3$ contents on the mineral crystallization of BFS was investigated by changing the composition of the BFS at the gas quenching temperature.

Based on the original composition of the BFS, the amounts of conditioning agents were reduced as much as possible to ensure full utilization of the waste heat of BFS and improve the value-added nature of the BFS. The experimental scheme is shown in Table II. $R$ ($R$ = = $1/M_k$) is defined as the mass ratio of the main basic oxides to the main acidic oxides in the BFS. This parameter is used to measure the chemical durability and stability of the BFS. The relation between $R$ and $M_k$ is given by Eq. (1):

$$R = \frac{\omega_{CaO} + \omega_{MgO}}{\omega_{SiO_2} + \omega_{Al_2O_3}} = \frac{1}{M_k} \quad (1)$$

where $R$ is the basicity of the BFS and defined as the mass ratio of the main basic oxides and acidic oxides in the slag; $M_k$ is the acidity of the BFS; $\omega$ is the mass fraction of the oxides in the BFS.

TABLE II. Experimental scheme ($m_{BFS}$ = 100 g)

| Group | Mass of conditioning agent, g | Variable | Content, % | | | |
|---|---|---|---|---|---|---|
| | | | CaO | MgO | $SiO_2$ | $Al_2O_3$ |
| 1 | – | BFS | 36.25 | 8.64 | 33.53 | 15.82 |
| 2 | 4.46 CaO | $R$ = 1.0 | 41.25 | 8.75 | 33.97 | 16.03 |
| 3 | 9.40 CaO | $R$ = 1.1 | 44.05 | 8.34 | 32.35 | 15.26 |
| 4 | 14.33 CaO | $R$ = 1.2 | 46.59 | 7.96 | 30.88 | 14.57 |
| 5 | 4.52 $SiO_2$ | $M_k$ = 1.2 | 36.71 | 8.75 | 38.53 | 16.02 |
| 6 | 9.01 $SiO_2$ | $M_k$ = 1.3 | 35.11 | 8.37 | 41.20 | 15.32 |
| 7 | 13.50 $SiO_2$ | $M_k$ = 1.4 | 33.65 | 8.02 | 43.65 | 14.68 |
| 8 | 1.51 MgO | $w$(MgO) = 10 % | 35.71 | 10.00 | 33.03 | 15.58 |
| 9 | 2.65 MgO | $w$(MgO) = 11 % | 35.31 | 11.00 | 32.66 | 15.41 |
| 10 | 1.42 $Al_2O_3$ | $w$($Al_2O_3$) = 17 % | 35.74 | 8.52 | 33.06 | 17.00 |
| 11 | 2.66 $Al_2O_3$ | $w$($Al_2O_3$) = 18 % | 35.31 | 8.42 | 32.66 | 18.00 |

As shown in Table II, the experimental scheme explores the influence of the composition of the BFS on mineral crystallization and the crystallization temperature in the granulation process in BFS by gas quenching using the FactSage 7.1 program. The influence of basicity, acidity, MgO content and $Al_2O_3$ content on mineral crystallization of BFS was explored. Groups 1–4 explore the influence of the basicity of the BFS; groups 5–7 explore the influence of the acidity of the BFS; groups 8–9 explore the influence of the MgO content of the BFS; groups 10–11 explore the influence of the $Al_2O_3$ content in the BFS. The basis of calculation is 100 g of BFS using the FactSage program.

*Thermodynamic simulation*

Thermodynamic simulations were performed using FactSage 7.1.[10,11] According to the composition of the BFS, the Foxide database was selected in the thermodynamic simulation. The Equilib module calculated the equilibrium state of the BFS at different temperatures, and the Phase Diagram module was used to simulate the mineral crystallization of the BFS to explain the mechanisms of mineral phase formation. All calculations were realized under a constant pressure of 1 atm. The temperature ranged from 1273 to 2073 K at 25-K increments.

*Experimental methods*

*Remelting experiments*. Remelting experiments were performed with high-temperature directional solidification cooling equipment (SK16-BYL); a silicon–molybdenum rod was used to heat and the maximum operation temperature was 1800 °C. The samples were cooled by circulating cooling water to maintain the minerals phases at the experimental temperature. Finally, the effect law of the BFS composition on minerals phases was investigated. The samples were dried for 6 h at 383 K in an air-drying oven. The temperature control program was set as follows: the heating rate was set at 25 K $min^{-1}$ and lasted for 63 min, raising the temperature from 298 to 1873 K during the heating period. In the constant-temperature period, the temperature remained at 1873 K for 60 min to remelt the samples completely. In the cooling period, the cooling rate was set to –1 K $min^{-1}$ from 1873 to 1623 K. In the second constant-temperature period, the furnace was held at 1623 K for 120 min to guarantee thermodynamic equilibrium. Finally, the samples were immersed in water to quench and preserve the mineral phases at the target temperature.

*XRD Analysis*

X-Ray diffraction (XRD) analysis was performed on powder samples (ground by a ZHM-1-P03061808). The XRD spectra were collected at 298 K using an X-ray diffractometer equipped with $CuK_{\alpha}$ radiation ($\lambda$ = 0.15405 nm). The voltage and current were 40.0 kV and 100.0 mA, respectively. All diffraction profiles were obtained in the continuous mode in the $2\theta$ range from 10 to 80° at a scan speed of 2° $min^{-1}$.

*SEM Analysis*

The morphology of the samples was assessed by scanning electron microscopy (SEM) on a field-emission scanning electron microscope (S-4800, Hitachi). The SEM images were taken at a magnification of 2000×.

## RESULTS AND DISCUSSION

The main components of BFS are $SiO_2$, CaO, $Al_2O_3$ and MgO, according to Table I. Due to the limitation of the computing power and the software database, only the influence of the four main oxides on the BFS phase was considered in the simulation calculations. The phase diagram module of the thermodynamic software FactSage 7.1 was used to construct Fig. 1.

As shown in Fig. 1, the area of the BFS in the phase diagram was determined according to the BFS composition. Melilite, anorthite, and spinel phases were generated during the crystallization process.

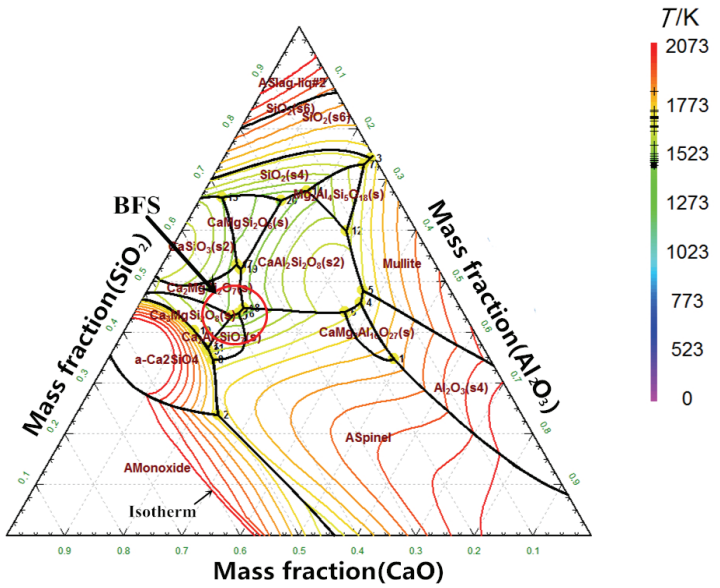


Fig. 1. Phase diagram of $SiO_2$–$Al_2O_3$–CaO–MgO ($\omega_{MgO}$ = 8.64 mass %) obtained using FactSage 7.1.

The crystallization temperature and the type, and amount of the minerals formed at various temperatures were simulated and calculated using the Equilib

module of FactSage 7.1. The basicity, acidity, and MgO and $Al_2O_3$ contents, were adjusted in order to estimate the mineral crystallization and crystallization temperature in the samples during the cooling process.

*Influence of basicity on mineral crystallization*

As shown in Fig. 2, melilite crystallized first at 1698.3 K while spinel and anorthite gradually crystallized with decreasing temperature. The initial crystallization temperature of the BFS increased from 1698.3 to 1892 K as the basicity was increased. The initial crystalline phase of the BFS was changed from melilite minerals to $\alpha$-$C_2S$ when the basicity was increased to 1.1.

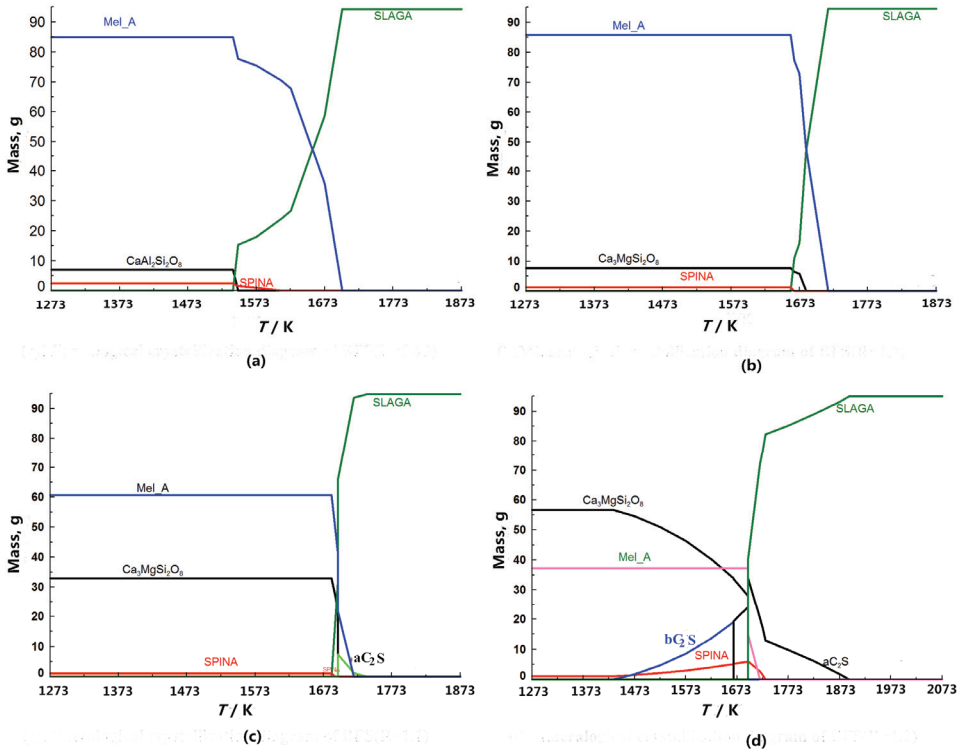


Fig. 2. Mineral crystallization diagrams of the BFS with different basicity: a) 0.91; b) 1.0; c) 1.1; d) 1.2. SLAGA stands for the liquid content of the BFS, SPINA for spinel, Mel_A for melilite minerals, $CaAl_2Si_2O_8$ for anorthite, $Ca_3MgSi_2O_8$ for manganolite and $\alpha$-$C_2S$ and $\beta$-$C_2S$ for dicalcium silicate).

Due to the instability of $\alpha$-$C_2S$, manganolite was then formed by the combination of $\alpha$-$C_2S$ and $Mg^{2+}$, which resulted in the disappearance of $\alpha$-$C_2S$ and the increase of manganolite with decreasing temperature. Increasing the basicity restrained the crystallization of melilite and anorthite, and promoted the crystal-

lization of manganolite and $\alpha$-$C_2S$. In summary, increasing the BFS basicity raised the initial crystallization temperature and changed the initial crystalline phase of the BFS. The large amount of the mineral phase was not conducive to the production of amorphous BFS beads. In order to understand further the effects of basicity on the mineral phase, a phase diagram of BFS was drawn with FactSage 7.1 and is shown in Fig. 3.

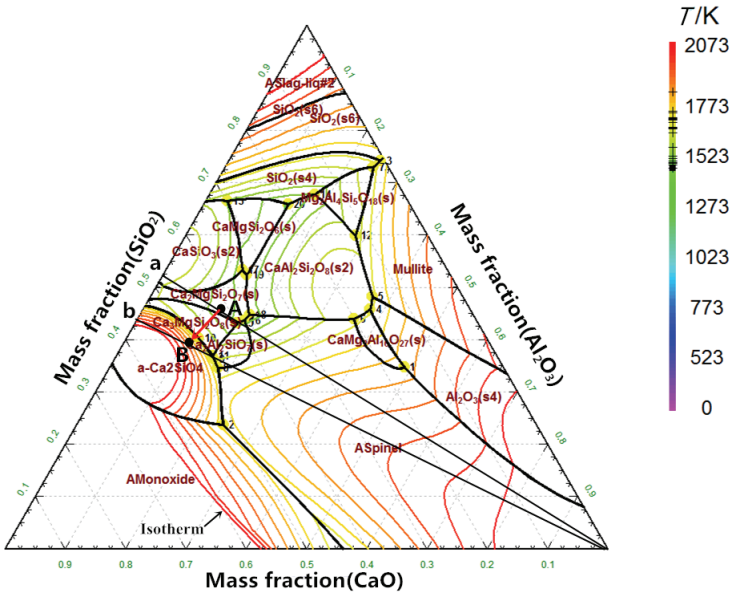


Fig. 3. Phase diagram of the BFS of different basicity. Point A represents the composition of the BFS with a basicity of 0.91 and B represents the composition of the BFS with a basicity of 1.2.

As shown in Fig. 3, the basicity at point A was 0.91 and the basicity at point B was 1.2. The change in the BFS composition from point A to point B was determined by quenching and tempering the samples. The composition of the mineral phase of the samples was changed from an initial crystalline phase of melilite to manganolite and $\alpha$-$C_2S$. From the temperature strip on the right, it could be see that the isotherm of point A was lower than that of point B. Therefore, the crystallization temperature of the solid phase increased as the basicity increased from 0.91 to 1.2. When the basicity of the BFS increased to 1.0, free $Ca^{2+}$ combined with the anorthite forming melilite; the $Ca^{2+}$ also combined with akermanite, thereby promoting the emergence of manganolite. When the basicity was increased further to 1.1, there was more free $Ca^{2+}$ in the BFS, which formed the $\alpha$-$C_2S$ phase with $Si^{2+}$ at high temperatures and raised the initial crystallization temperature. As shown in Figs. 2 and 3, the initial crystallization temperature

increased and was controlled by the precipitation of melilite, when the basicity increased from 0.91 to 1.0. The initial crystallization temperature increased again when the basicity was increased from 1.1 to 1.2, which was determined by $\alpha$-$C_2S$. This means that increasing the basicity led to a higher crystallization temperature in the BFS.

*Influence of acidity on mineral crystallization*

It could be seen from Fig. 4 that melilite crystallized first at 1698.3 K, and spinel and anorthite gradually crystallized with decreasing temperature. The crystallization temperature of the BFS decreased from 1698.3 to 1581.4 K with increasing acidity.

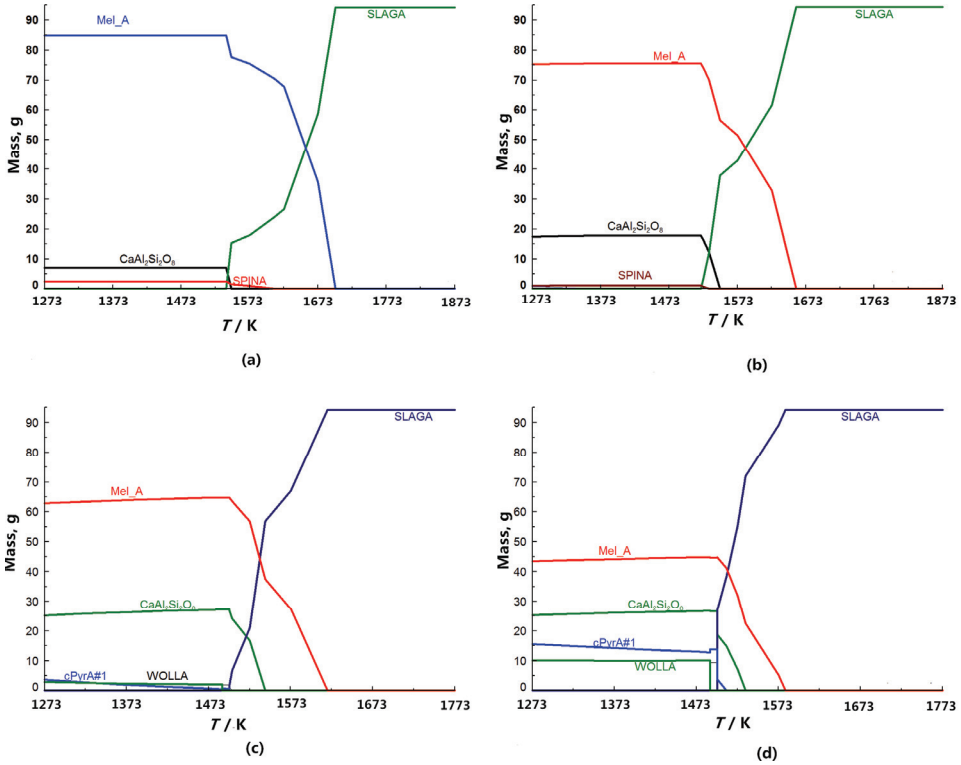


Fig. 4. Mineral crystallization diagram of the BFS with different acidity (basicity): a) 1.1; b) 1.2; c) 1.3; d) 1.4). SLAGA stands for liquid BFS, Mel_A for melilite minerals, SPINA for spinel, $CaAl_2Si_2O_8$ for anorthite, cPyrA#1 for pyroxene minerals and WOLLA for wollastonite minerals.

Pyroxene minerals and wollastonite minerals crystallized and spinel disappeared when the acidity was increased to 1.3. Increasing the acidity retained the crystallization of melilite minerals and anorthite, and promoted the crystallization

of pyroxenes and wollastonite minerals. In summary, increasing the acidity caused the initial crystallization temperature to decrease and the degree of crystallization to be reduced, which is conducive to the production of amorphous BFS beads. Increasing the amorphous content raises the activity of the BFS beads allowing them to be widely used in the field of building materials and improving the value-added nature of the BFS byproduct. In order to understand further the effects of acidity on the formation of mineral phases, the phase diagram of the BFS was drawn with FactSage 7.1 and is shown in Fig. 5.

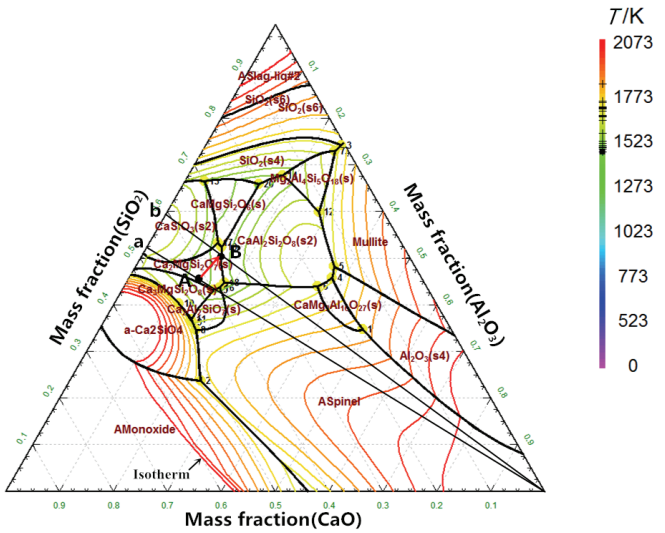


Fig. 5. Phase diagram of BFS of different acidity. A represents the composition of the BFS with an acidity of 1.1 and B represents the composition of the BFS with an acidity of 1.4.

As shown in Fig. 5, the acidity at point A was 1.1 and the acidity at point B was 1.4. The change in the BFS composition from point A to point B was determined by quenching and tempering the samples. The mineral phases of the samples changed from the initial crystalline phase of akermanite to anorthite. From the temperature strip on the right, it could be see that the isotherm of point A was higher than that of point B. Therefore, the crystallization temperature decreased as the acidity increased from 1.1 to 1.4. Increasing the $SiO_2$ content caused the melilite to release $Ca^{2+}$, which led to a decrease in the content of melilite minerals and an increase in anorthite. As shown in Figs. 4 and 5, the crystallization temperature was determined by melilite and the conversion of the acid oxides, $SiO_2$ and $Al_2O_3$, into crystals required more energy, which restrained the crystallization of the BFS.[12] On the other hand, the CaO and MgO contents were relatively decreased, but not enough to provide conditions for crystal formation. Therefore, from the crystallization temperature, it is known that

increasing the BFS acidity decreased the initial crystallization temperature and reduced the amount of mineral phases, even to the point of having no crystallization of the mineral phases at the gas quenching temperature.

*Influence of MgO content on mineral crystallization*

Fig. 6 shows that the crystallized minerals were melilite, spinel, and anorthite after the addition of the conditioning agent MgO. The crystallization temperature of the BFS decreased slightly and the initial crystalline phase changed from melilite to spinel with increasing amounts of MgO. In summary, the crystallization amount of the melilite phase was almost unchanged and increasing the MgO content promoted the crystallization of spinel and restrained the crystallization of the anorthite phase. In order to understand further the effects of the MgO content on the mineral phases, the phase diagram for the BFS was drawn with FactSage 7.1 and shown in Fig. 7.

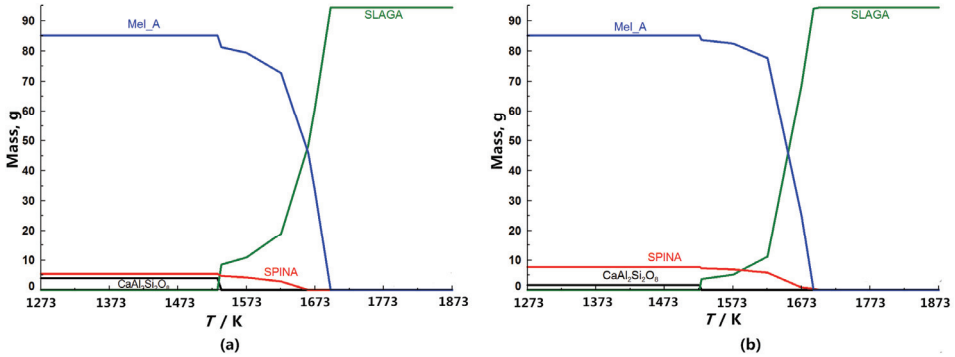


Fig. 6. Mineral crystallization diagram of BFS with varying contents of MgO: a) 10; b) 11 %. SLAGA stands for liquid BFS, Mel_A for melilite minerals, SPINA for spinel and $CaAl_2Si_2O_8$ for anorthite.

As shown in Fig. 7, the MgO content at point A was 8.64 mass % and at point B was 11 mass %. The change in the BFS composition from point A to point B was determined by quenching and tempering the samples. The samples were in the initial crystallization field melilite, and the main crystalline phases of the samples were melilite, spinel and anorthite. From the temperature strip on the right, it could be seen that the isotherm of point A is slightly higher than that of point B. Therefore, the initial crystallization temperature of the solid phase decreased as the MgO content increased from 8.64 to 11 mass %. Increasing the MgO content shifted the sample away from the initial crystallization field of melilite to spinel, which led to a decrease in the amount of the melilite phase, promoted the crystallization of the spinel phase and decreased the crystallization temperature. As shown in Figs. 6 and 7, the crystallization temperature of the BFS was determined by the crystallization of melilite when the MgO content was

increased from 8.64 to 10 mass %. The crystallization temperature of the BFS was determined by the crystallization of spinel when the MgO content was increased to 11 mass %. Adjusting the MgO content showed little change in the amount of crystalline phases in the BFS, thereby rendering this parameter ineffective for the preparation of amorphous BFS beads.

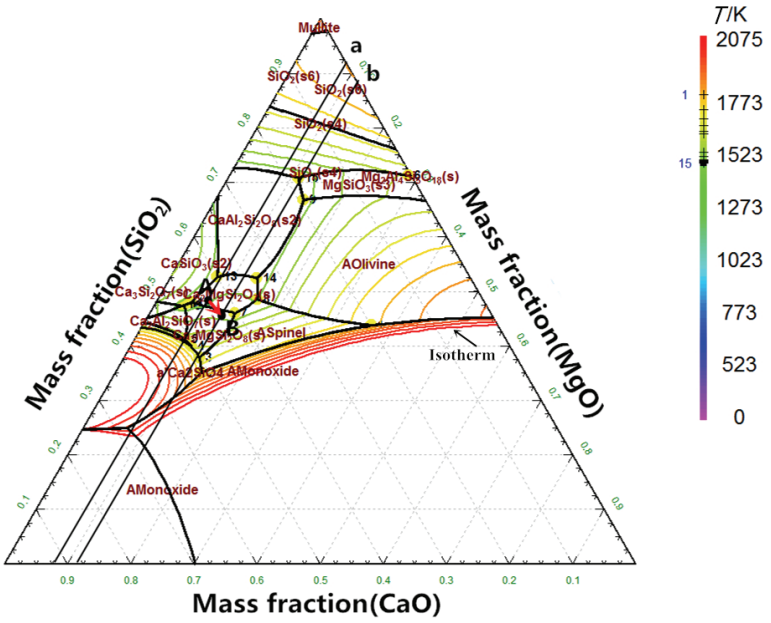


Fig. 7. Phase diagram of the BFS with varying contents of MgO (A and B represent the compositions of the BFS with 8.64 and 11 mass % MgO, respectively).

*Influence of $Al_2O_3$ content on mineral crystallization*

After addition of the conditioning agent $Al_2O_3$, the crystallized minerals were melilite, spinel, and anorthite, as shown in Fig. 8. With increasing $Al_2O_3$ content, the initial crystalline phases were melilite minerals, and the initial crystallization temperature of the BFS was only slightly increased from 1698.3 to 1710.1 K, according to the calculation of Equilib module. In summary, increasing the $Al_2O_3$ content restrained the crystallization of the melilite phase and promoted the crystallization of spinel and anorthite. In order to understand further the effects of the $Al_2O_3$ content on the mineral phases, the phase diagram of the BFS was drawn with FactSage 7.1, and shown in Fig. 9.

As could be seen in Fig. 9, the $Al_2O_3$ content at point A was 15.82 mass % and at point B, it was 18 mass %. The change in the BFS composition from point A to point B was determined by quenching and tempering the samples.

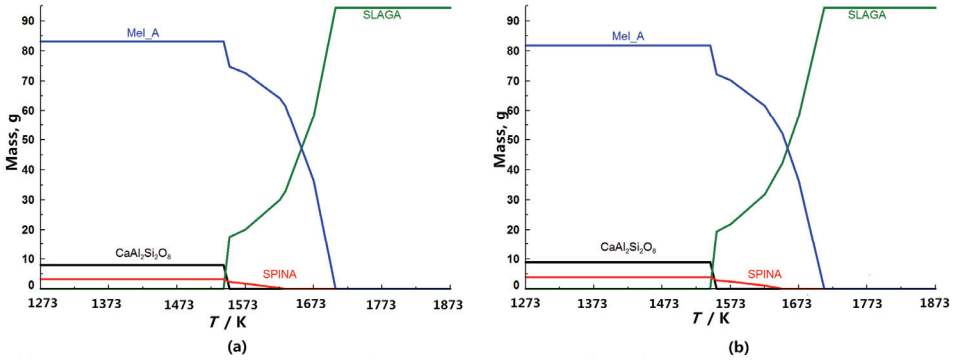


Fig. 8. Mineral crystallization diagram of BFS with varying $Al_2O_3$ contents: a) 17; b) 18 %. SLAGA stands for liquid BFS, Mel_A for melilite minerals, SPINA for spinel, $CaAl_2Si_2O_8$ for anorthite.

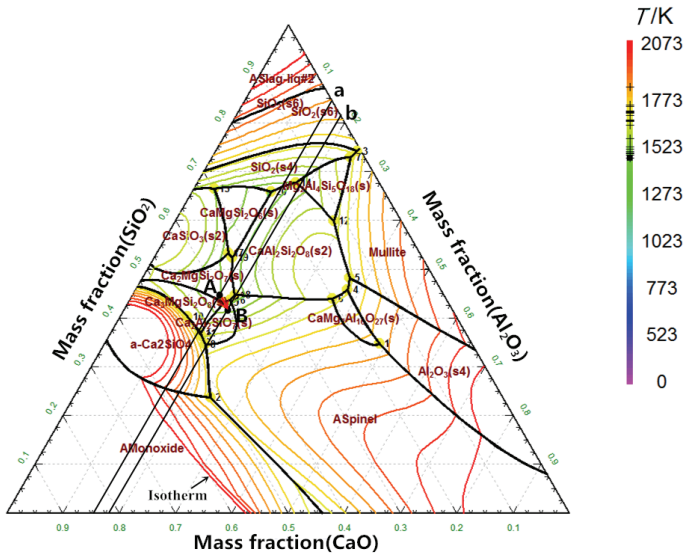


Fig. 9. Phase diagram of the BFS with varying $Al_2O_3$ contents (A and B represent the compositions of the BFS with 15.82 and 18 mass % MgO, respectively).

The samples were initially in the crystallization field of melilite to spinel, which is conducive for the crystallization of spinel. The main phases of the samples were melilite, spinel, and anorthite with different $Al_2O_3$ content. As the $Al_2O_3$ content increased from 15.82 to 18 mass %, the isotherm of point A was found to be slightly lower than that of point B from the temperature strip on the right. Therefore, the initial crystallization temperature of the solid phase increased as the $Al_2O_3$ content increased from 15.82 to 18 mass %. By increasing the $Al_2O_3$ content, a large amount of melilite phase and a small amount of spinel

phase would crystallize; therefore, it was not conducive to the preparation of amorphous BFS beads.

*XRD and SEM results*

The amount of mineral crystallization should be decreased as much as possible in order to obtain a high activity amorphous BFS beads, which could result in a high value-added utilization of BFS.[13–15] Increasing the BFS acidity effectively reduces the crystallization temperature of the BFS. This was especially true when the acidity was increased to 1.3, leading to an initial crystallization temperature lower than 1623 K, which satisfies the requirements for the preparation of amorphous BFS beads. Slag remelting experiments were performed with different acidities and the samples were analyzed by XRD and SEM to verify the simulation results of the thermodynamic software FactSage 7.1.

As shown in Figs. 10 and 11, the XRD patterns for sample $M_k$ = 1.1 exhibited akermanite, gehlenite, and spinel, and the SEM micrograph of the sample clearly showed the original crystalline phase of the sample with the size of crystalline phase ranging from 0.3 to 2.8 mm. The XRD patterns and SEM micrographs show that sample $M_k$ = 1.1 had large amounts of crystalline akermanite, gehlenite, and spinel phases.

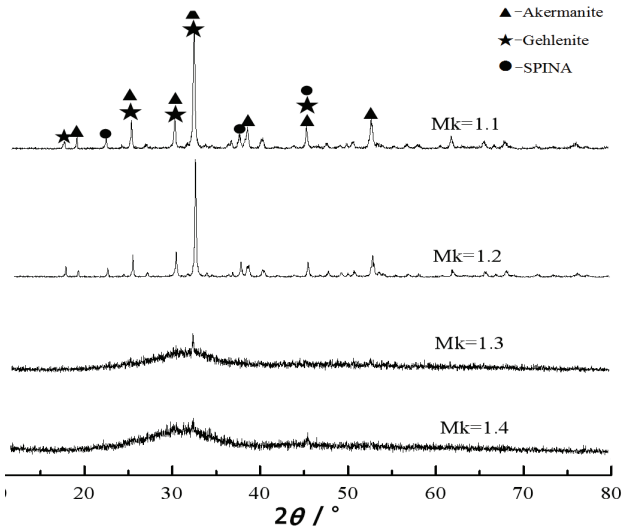


Fig. 10. X-Ray diffraction patterns of BFS samples of different acidity, $M_k$ (phases detected: ▲- akermanite; ✱ - gehlenite and ● - spinel).

The XRD patterns for sample $M_k$ = 1.2 showed the same types of crystalline phase as those present in the $M_k$ = 1.1 sample. However, the SEM micrographs showed that the crystallization field became smaller with the size of the crystalline phase ranging from 0.02 to 0.08 mm. The XRD patterns and SEM micro-

graphs showed that the amount of crystalline phase of sample $M_k$ = 1.2 decreased and the size of the crystalline phase became smaller. When the acidity of the sample was increased to 1.3, the XRD patterns showed weak diffraction peaks for akermanite, while the SEM micrographs barely revealed any crystalline phase. When the acidity of the samples was increased to 1.4, the XRD patterns of the samples were broad and basically devoid of peaks, indicating that they were in the amorphous state. The SEM micrographs did not evidence any crystalline phase, showing instead a smooth and uniform surface. The XRD patterns and SEM micrographs reveal that the amounts of the crystalline phases decreased and then disappeared when increasing the acidity. Thus, the simulation results, from the thermodynamic software FactSage 7.1 were verified by the XRD and SEM results.

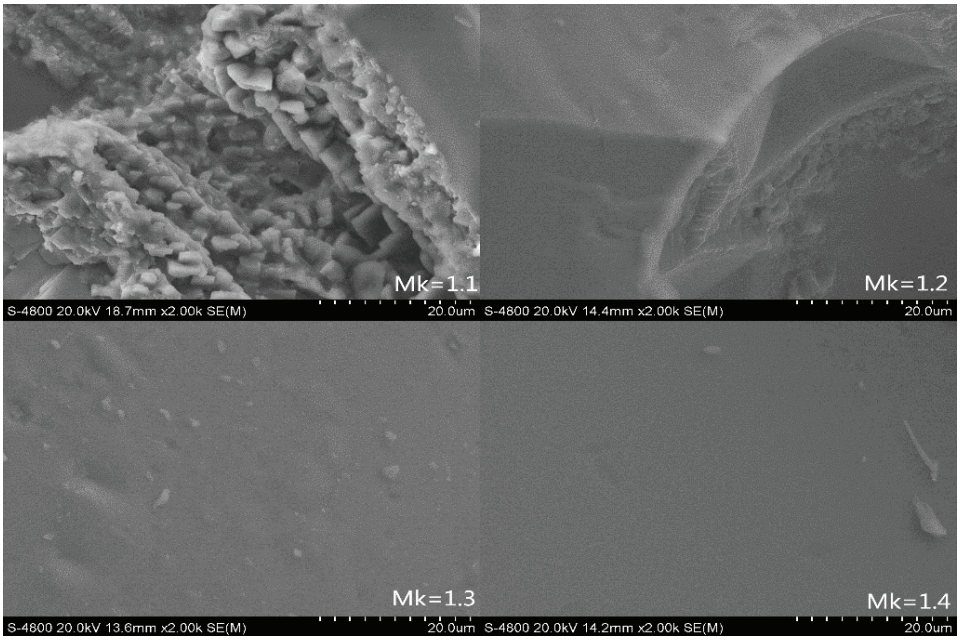


Fig. 11. SEM micrographs of BFS samples of different acidity, $M_k$ ($M_k$ ranging from 1.1 to 1.4).

## CONCLUSION

The following can be concluded from this study on the influence of basicity, acidity, MgO content, and $Al_2O_3$ content on the crystallization of BFS. With the increasing basicity, the crystallization temperature increased and the degree of crystallization increased at the gas quenching temperature, which was not conducive to producing amorphous BFS beads. Increasing the MgO and $Al_2O_3$ contents had little effect on the crystallization temperature or the amount of crystallization, which did not aid in the production of amorphous BFS beads. Fortun-

ately, the crystallization temperature significantly decreased with increasing acidity from 1.1 to 1.4. Additionally, the BFS was amorphous at the gas quenching temperature with no mineral crystallization when the acidity was higher than 1.3, which is conducive to the production of amorphous BFS beads.

*Acknowledgement.* This research was supported by the National Key Research and Development Project (2016YFB0601403).

И З В О Д

## ПРОУЧАВАЊЕ КРИСТАЛИЗАЦИЈЕ МИНЕРАЛА ПРИ ГРАНУЛАЦИЈИ ГАСОМ ШЉАКЕ ВИСОКИХ ПЕЋИ

KANG YUE1, LIU CHAO[1], ZHANG YUZHU[1, 2], XING HONGWEI[2], LONG YUE[2] и JIANG MAOFA[1]

[1]*School of Metallurgy, Northeastern University, 110819, Shenyang , China,* [2]*College of Metallurgy and Energy, North China University of Science and Technology, 063009, Tangshan , China*

Процес гранулације шљаке високе пећи (BSF, односно ШВП) брзим хлађењем гасом омогућава ефикасно искоришћење отпадне топлоте ШВП и повећање вредности споредних продуката ШВП. Са снижењем температуре, ШВП кристалише у мелилит, анортит, спинел, итд. Кристализација ових минерала, међутим, не погодује добијању аморфних ШВП гранула. У овом истраживању је примењена термодинамичка симулација и експерименти поновног топљења да би се испитао утицај базности, киселости и садржаја MgO и $Al_2O_3$ у ШВП на кристализацију. Кристализација током брзог хлађења гасом се може спречити контролом састава ШВП. Резултати показују да повећање базности ШВП доводи до рапидног повишења температуре кристализације, а одигравање кристализације на вишим температурама није погодно за формирање аморфне фазе. Повећање киселости ШВП може значајно да снизи температуру кристализације; када је киселост повећана до 1,3, аморфне грануле ШВП су добијене на температури брзог хлађења гасом (1623 K). Иако је повећање садржаја MgO и $Al_2O_3$ у ШВП имало мали утицај на температуру кристализације и принос, добијање аморфних гранула ШВП брзим хлађењем гасом се може реализовати подешавањем киселости ШВП.

(Примљено 12. децембра 2017, ревидирано 22. маја, прихваћено 31. маја 2018)

## REFERENCES

1. Z. Hui, W. Hong, Z. Xun, J. Q. Yong, L. Kai, C. Rong, L. Qiang, *Appl. Energy* **112** (2013) 956
2. J. X. Liu, Q. B. Yu, Z. L. Zuo, F. Yang, W. J. Duan, Q. Qin, *Constr. Build. Mater.* **131** (2017) 381
3. G. Bisio, *Energy* **22** (1997) 501
4. Q. Q. Ren, Y. Z. Zhang, Y. Long, S. S. Chen, Z. S. Zou, J. Li, C. G. Xu, *J. Iron Steel Res. Int.* **24** (2017) 601
5. X. T. Dai, Y. H. Qi, C. X. Zhang, H. C. Xu, D. L. Yan, Y. C. Hong, *J. Iron Steel Res.* **19** (2007) 14
6. X. P. Yang, *Modern Metallurgy* **42** (2014) 37
7. J. X. Liu, Q. B. Yu, P. Li, C. X. Dou, X. Z. Hu, *Iron Steel* **45** (2010) 95 (doi: 10.13228/j.boyuan.issn0449-749x.2010.02.032)
8. X. Zhu, H. Zhang, Y. Tan, H. Wang, Q. Liao, *Appl. Therm. Eng.* **88** (2015) 157
9. S. J. Pickering, N. Hay, T. F. Roylance, G. H. Thomas, *Ironmak. Steelmak.* **12** (1985) 14
10. C. Liu, Y. Z. Zhang, J. Li, J. G. Li, Y. Kang, *SpringerPlus* **5** (2016) 1

11. Z. M. Cao, X. Y. Song, Z. Y. Qiao, *Chin. J. Rare Metals* **32** (2008) 216 (doi: 10.13373/j.cnki.cjrm.2008.02.026)
12. L. F. Ding, W. Ning, Q. W. Wang, D. N. Shi, L. D. Luo, *Mater. Lett.* **141** (2015) 327
13. A. A. Francis, *J. Eur. Ceram. Soc.* **24** (2004) 2819
14. J. I. Escalante, L. Y. Gomez, K. K. Johal, K. Mendoza, H. Mancha, J. Mendez, *Cem. Concrete Res.* **31** (2001) 1403
15. J. Lee, K. Yabuta, A. Hayashi, K. Morita, *ISIJ International* **43** (2003) 2073.